Fluoride Inhibition of Yeast Enolase. 2. Structural and Kinetic Properties of the Ligand Complexes Determined by Nuclear Relaxation Rate Studies†

Thomas Nowak*,‡ and Peter J. Maurer

ABSTRACT: The formation of inhibitory complexes of enolase–Mn with fluoride ion (F^-) and with orthophosphate has been thermodynamically characterized [Maurer, P. J., & Nowak, T. (1981) *Biochemistry* (preceding paper in this issue)]. In the present study, the kinetic constants and the structures of these complexes have been obtained by ^{19}F and ^{31}P nuclear relaxation studies. These ligands can interact independently to form their respective ternary enzyme–Mn–ligand complexes, and the ligands can bind with mutual cooperativity to form a quaternary enolase–Mn–F–P_i complex. The normalized paramagnetic relaxation rate values for ^{19}F in the ternary E–Mn–F complex measured at 30 °C and at 94.1 MHz are $1/pT_{1p} = 2.6 \times 10^6$ s^{-1} and $1/pT_{2p} = 3.5 \times 10^6$ s^{-1}. These values are a measure of chemical exchange as suggested by the relaxation rate ratio and by the Arrhenius behavior of the relaxation rates measured vs. temperature. The formation of the quaternary complex, upon addition of P_i, decreases the ^{19}F relaxation rates ($1/pT_{1p} = 4.5 \times 10^4$ s^{-1} and $1/pT_{2p} = 5.2 \times 10^4$ s^{-1}), indicating a decrease in the ^{19}F ligand exchange rate. The relaxation rates are decreased in a competitive manner upon the addition of the substrates P-enolpyruvate and D(+)-2-phosphoglycerate, indicating competition between F^- and substrate. The activation parameters for ^{19}F exchange have been determined. These values are $\Delta H^\ddagger = 11.0$ kcal/mol, $T\Delta S^\ddagger = 2.33$ kcal/mol, and $\Delta H^\ddagger = 11.6$ kcal/mol, $T\Delta S^\ddagger = 1.3$ kcal/mol for the ternary and quaternary complexes, respectively. From the values of $1/pT_{1p}$, an upper limit to the Mn–F distance, r, can be calculated. The Mn–F distance in the ternary complex is <2.3 Å, and in the quaternary complex, $r < 4.3$ Å. It is assumed that the F^- interacts in the primary coordination sphere of the enolase-bound Mn^{2+} in both the ternary and quaternary complexes. The ^{31}P relaxation rates were measured at 40.5 MHz at 30 °C for the ternary and quaternary complexes. The $1/pT_{1p}$ values for the ternary complex ($1/pT_{1p} = 3.96 \times 10^3$ s^{-1}) and the quaternary complex ($1/pT_{1p} = 1.13 \times 10^3$ s^{-1}) both show Arrhenius behavior; however, the $1/pT_{2p}$ values are approximately an order of magnitude larger. A strong frequency dependence of $1/pT_{1p}$ of ^{31}P for both complexes demonstrates that $1/pT_{1p}$ is a measure of relaxation ($1/T_{1M}$). The frequency dependence of $1/pT_{1p}$ was also used to determine the distribution of Mn^{2+} under experimental conditions in the enzyme–Mn complexes which contain P_i. The frequency dependence of $1/T_{1M}$ was used to determine the correlation times (τ_c) for the Mn–^{31}P interactions in the ternary ($\tau_c = 9 \times 10^{-9}$ s) and quaternary ($\tau_c = 6 \times 10^{-9}$ s) complexes. These τ_c values are similar to other values estimated for enolase–Mn complexes. The Mn–^{31}P distance, r, is shown to increase from 6.5 Å in the ternary enolase–Mn–P_i complex to 7.7 Å in the quaternary enolase–Mn–F–P_i complex. These data demonstrate that P_i does not bind in the primary coordination sphere of the bound Mn^{2+} and that a conformational change occurs upon binding of F^- which increases the value of r for P_i. The dissociation constant of Mn^{2+} to enolase ($K_d = 10$ μM) decreases in the presence of P_i to 3 μM and decreases even further in the presence of P_i and F^- ($K_d = 0.3$ μM). The inhibition of enolase by F^- and P_i has been demonstrated to occur by the formation of a tightly bound, and thus slowly exchanging, complex containing enzyme–Mn–F–P_i. The F^- interacts directly with the cation which is at the catalytic site and serves as a possible analogue of the attacking OH^- group. The P_i is bound at the coordination site for the phosphoryl group of the substrate and is in an outer sphere complex with the bound Mn^{2+}. Because of the potency of inhibition, it is suggested that this quaternary complex induces a transition state like complex of the enzyme.

Fluoride ion has been found to be a potent inhibitor of some enzyme systems such as succinate dehydrogenase and pyrophosphatase (i.e., Slater & Bonner, 1952; Bayakov et al., 1976) and an activator of others such as adenylate cyclase (i.e., Keirns et al., 1973; Ross & Gilman, 1980). A classic example of fluoride inhibition is its potent inhibition of glycolysis, specifically, its action on the enzyme enolase. This potent inhibition was shown to be manifested in the presence of P_i,[1] an intracellular, physiological buffer (Warburg & Christian, 1941–1942). This complex inhibition was shown kinetically to be due to a cooperative effect between the interaction of F^- and of P_i to the enolase–cation complex. The kinetic constants for this inhibition have been determined for enolase from rabbit muscle (Wang & Himoe, 1974).

Enolase isolated from yeast has been studied as the enolase–Mn^{2+} complex with respect to the interactions of F^- and P_i in the previous paper of this issue (Maurer & Nowak, 1981). It was demonstrated that enolase–Mn–ligand ternary complexes are formed with F^- and with P_i. The ligand perturbs the environment of the bound Mn^{2+}, as reflected in a change in PRR enhancement of the resulting complex, and each ligand causes a perturbation of the protein structure, as reflected in a UV spectra change. The addition of both ligands to enolase–Mn results in the quaternary enzyme–Mn–F–P_i complex

† From the Department of Chemistry, Program in Biochemistry and Biophysics, University of Notre Dame, Notre Dame, Indiana 46556. *Received February 24, 1981; revised manuscript received July 15, 1981.* This work was supported in part from National Institutes of Health Research Grants AM17049 and AM00486, Biomedical Science Support Grant RR07033-10 from The General Research Resources, and a Grant-in-Aid from Miles Laboratories, Elkhart, IN. Support is also acknowledged to the Purdue University Biochemical Magnetic Resonance Laboratory and support from National Institutes of Health Grant RR01077 from The Division of Research Resources for the use of their NMR facilities.

‡ Recipient of Research Career Development Award AM00486 from the National Institutes of Health.

[1] Abbreviations used: P-enolpyruvate, phosphoenolpyruvate; 2-PGA, D(+)-2-phosphoglyceric acid; FID, free induction decay; P_i, orthophosphate; PP_i, inorganic pyrophosphate.

0006-2960/81/0420-6901$01.25/0

via a random pathway. Dissociation constants for each ligand decrease by more than 2 orders of magnitude in the presence of the second ligand to yield the tightly bound, strongly inhibited enzyme complex. The UV spectral changes of the quaternary complex indicate that an additional conformational change has been induced, and the PRR enhancement suggests that the bound Mn^{2+} becomes highly inaccessible to rapidly exchanging solvent molecules.

The data indicate that the F^- interacts directly with the bound Mn^{2+} and displaces one molecule of water. The enolase–Mn complex has been shown to have two water molecules coordinated to the bound Mn^{2+} (Nowak et al., 1973). The P_i alters the environment of the bound Mn^{2+} presumably via a complex where the P_i is hydrogen bonded to one of the metal-bound water molecules. In the quaternary complex, the exchange rate of the Mn^{2+}-bound water decreases, leaving the cation inaccessible to the bulk solvent.

This paper examines the effect of the bound Mn^{2+} on the nuclear relaxation rates of the F^- and P_i ligands by ^{19}F and ^{31}P NMR studies. These studies have been performed as a function of Mn^{2+} concentration and of temperature and frequency. The results of these studies have yielded values for the correlation time for the Mn–ligand interactions and led to a determination of the kinetic and structural parameters which describe the ternary and quaternary complexes. The data indicate that the F^- interacts directly with the bound Mn^{2+} in the formation of the ligand complex whereas P_i forms a second sphere complex with the cation. In the quaternary complex, the exchange rates of the ligands decrease considerably to form the highly inhibitory, slowly exchanging enolase–Mn–F–P_i complex. The structure of the inhibitory complex is analogous to the proposed catalytic complex and may be analogous in structure to the transition state of the reaction.

Material and Methods

Enolase was prepared from bakers' yeast as described (Westhead & McLain, 1964) with slight modifications (Maurer & Nowak, 1981). The enzyme was judged homogeneous by polyacrylamide gel electrophoresis and had a specific activity of 95–100% of that stated by Westhead & McLain (1964).

Trisodium D(+)-2-PGA and phosphoglycolate were obtained from Sigma. The reagents KCl, KF, KOH, KH_2PO_4, $MgCl_2 \cdot 6H_2O$, and $MnCl_2 \cdot 4H_2O$ were all reagent grade. Solutions of P_i were made by titrating KH_2PO_4 with KOH to the proper pH prior to final dilution.

When necessary, solutions (including solutions containing enzyme) were made metal free by passage through a Chelex-100 (Bio-Rad) resin column. This treatment was important in removing endogenous metal ion contaminants. Distilled deionized water was used routinely for all solutions.

The enzyme concentration was determined by using the extinction coefficient $\epsilon_{280} = 0.89$ mL mg^{-1} cm^{-1} (Warburg & Christian, 1941–1942) and the molecular weight of 88 000 per dimer (Mann et al., 1970). The enzyme was assayed as described by Westhead & McLain (1964) and modified (Maurer & Nowak, 1981). The formation of P-enolpyruvate was monitored by using a Gilford 240 spectrophotometer at 240 nm at 30 °C.

High-Resolution ^{19}F and ^{31}P Spectra. The ^{19}F spectra, obtained at 94.1 MHz, and the ^{31}P spectra, obtained at 40.5 MHz, were attained with a Varian XL-100-15 spectrometer interfaced with a TTI pulse system and a Nicolet 1080 computer. The spectrometer was field-frequency locked on internal ^2H present as ^2H_2O in the solvent. For variable temperature studies, the temperature was varied and measured as described for PRR studies (Maurer & Nowak, 1981). The $1/T_1$ values were measured by the inversion recovery method (Vold et al., 1968; Allerhand et al., 1971) and $1/T_2$ was estimated from the following relationship:

$$\frac{1}{T_2} = 2\pi(\nu_{1/2} - B) \tag{1}$$

where $\nu_{1/2}$ is the spectral line width at half-height in hertz and B is the artificial line broadening due to the exponential multiplication of the FID prior to Fourier transformation of the spectrum. Generally the value of B was 0.5 Hz.

In the Mn^{2+} titration experiments, microliter quantities of $MnCl_2$ solutions were titrated into buffered solutions of metal-free enzyme which contained the specific ligand(s) of interest. The relaxation rates were measured, $1/T_1$ and $1/T_2$ values were plotted against $[Mn^{2+}]$, and the slope, m, was determined. The normalized paramagnetic contribution to the relaxation rate, $1/pT_{np}$ ($n = 1$ or 2), was calculated from the expression

$$\frac{1}{pT_{np}} = m([L]_t + K_d) \tag{2}$$

where $[L]_t$ is the total ligand concentration and K_d is the dissocation constant for that ligand from the enzyme–Mn–ligand complex. The term K_d is ignored if $K_d \ll [L]$. Under these conditions, the normalization factor $1/P$ is equal to $[L]/[Mn^{2+}]$ (Mildvan & Cohn, 1970).

In an investigation of the paramagnetic effects of enzyme-bound Mn^{2+} on the nuclear relaxation rates of the ligand(s) which binds to the enzyme complex, one must be concerned with the distribution of the Mn^{2+} which is added to the solution. A contribution from binary Mn–ligand complexes must be determined and compensated for in order to correctly quantitate the relaxation rates of the nuclei of the ligands in the enzyme–Mn–ligand complex. For the experiments where the formation of the enzyme–Mn–F complex was investigated, a correction for binary Mn–F was obtained. A measure of the paramagnetic effect of Mn^{2+} on the relaxation rates of ^{19}F was made from a titration of Mn^{2+} into a solution of KF to form the binary Mn–F complex. This titration was performed at two F^- concentrations, and values for $1/pT_{np}$ and K_d were obtained for the binary complex from eq 2. In the presence of enzyme, the Mn^{2+} is distributed between the binary Mn–F and the ternary enzyme–Mn–F complexes. To simply estimate this distribution, the relaxation rates are measured as a function of added Mn^{2+}. The complete expression for the slope of the plot of the data, taking into account the Mn^{2+} distribution, yields the expression

$$m = \frac{(f)_f\left(\frac{1}{pT_{np}}\right)_{MF}}{K_{d_{MF}} + [F^-]} + \frac{(f)_b\left(\frac{1}{pT_{np}}\right)_{EMF}}{K_{d_{EMF}} + [F^-]} \tag{3}$$

In eq 3, $(f)_b$ is the fraction of Mn^{2+} bound to the enzyme, and $(f)_f$ is the fraction of Mn^{2+} not enzyme bound. The subscripts MF and EMF refer to the respective binary and ternary complexes.

Determination of the Distribution of Mn^{2+} by a Frequency Dependence of $1/T_{1p}$ of ^{31}P. In the previous method of determining the distribution of Mn^{2+} among ligand complexes, one must know the dissociation constant for metal in the E–M–L complex. For some ternary and higher complexes, such values are neither known nor easily measurable (i.e., Nowak & Lee, 1977). The binding of Mn^{2+} to enolase is not

significantly affected by the presence of F^-; however, the presence of P_i or P_i and F^- increases the binding of Mn^{2+} to enolase. Accurate quantitative values were not directly obtained by EPR techniques (P. J. Maurer and T. Nowak, unpublished observations). A determination of the distribution of Mn^{2+} among complexes can be performed from a frequency dependence of the paramagnetic effect of the relaxation rates.

If experimental conditions are controlled such that $[L] \gg K_{d_{ML}}$, $K_{d_{EML}}$, and n is the fraction of Mn^{2+} bound to the enzyme, then

$$\left(\frac{1}{pT_{1p}}\right)_{obsd} = n\left(\frac{1}{pT_{1p}}\right)_{EML} + (1-n)\left(\frac{1}{pT_{1p}}\right)_{ML} \quad (4)$$

where $(1/pT_{1p})_{obsd}$ is the observed normalized relaxation rate of the nucleus of the ligand. From the Swift–Connick (1962) equations, where

$$\frac{1}{pT_{1p}} = \frac{1}{T_{1M} + \tau_M} \quad (5a)$$

$$\frac{1}{pT_{2p}} = \frac{1}{T_{2M} + \tau_M} \quad (5b)$$

(Swift & Connick, 1962; Luz & Meiboom, 1964), the values T_{1M} and T_{2M} refer to the relaxation times of the nuclei of the ligands in the metal complex, and τ_M is the mean residence time of the ligand in the metal complex. When $\tau_M > T_{nM}$, then observed relaxation is dominated by chemical exchange (slow exchange). If $\tau_M \ll T_{nM}$, then the observed relaxation is dominated by nuclear relaxation (fast exchange) where $1/pT_{1p} = 1/T_{1M}$. The longitudinal relaxation rate of the nucleus is described by the Solomon–Bloembergen equation (Solomon, 1955; Bloembergen, 1957) as simplified by Mildvan & Engle (1972) as

$$\frac{1}{T_{1M}} = \left(\frac{c}{r}\right)^6 f(\tau_c) \quad (6)$$

where r is the electron-nuclear distance (metal-nucleus distance) of the complex under investigation, c is a collection of constants, and $f(\tau_c)$ is a correlation time function. The correlation time function has the following form:

$$f(\tau_c) = \frac{3\tau_c}{1 + \omega_I^2\tau_c^2} + \frac{7\tau_c}{1 + \omega_s^2\tau_c^2} \quad (7)$$

where ω_I is the nuclear precession frequency and ω_s is the electron precession frequency. The correlation time τ_c is the time constant for the physical process which modulates the electron-nuclear interaction and is related to three processes.

$$\frac{1}{\tau_c} = \frac{1}{\tau_m} + \frac{1}{\tau_r} + \frac{1}{\tau_s} \quad (8)$$

In eq 8, τ_m is the mean residence time of the nucleus of the ligand in the environment of the paramagnetic ion, τ_r is the rotational correlation time of the ion–ligand complex, and τ_s is the electron spin relaxation time of the paramagnetic species.

For determination of the distribution of Mn^{2+} in complexes containing P_i, a frequency dependence of the paramagnetic effect of Mn^{2+} on $1/T_1$ of ^{31}P was performed. Since the correlation time of the binary Mn–P_i complex is short ($\tau_c = \tau_r \approx 2 \times 10^{-11}$ s), it is assumed that $(1/T_{1M})_{ML}$ is frequency independent over the frequency range measured (a 0.2% change is expected). If $1/pT_{1p}$ for the ternary complex is in fast exchange, a frequency dependence of relaxation rates would be expected (see above). Thus from eq 4 and 6, we can solve for τ_c, assuming τ_c is frequency independent over the frequencies of observation, to yield

$$\tau_c^2 = \left[\left(\frac{1}{pT_{1p}}\right)_2 - \left(\frac{1}{pT_{1p}}\right)_1\right] \Big/ \left[\omega_{I1}^2\left(\frac{1}{pT_{1p}}\right)_1 - \omega_{I2}^2\left(\frac{1}{pT_{1p}}\right)_2 + (\omega_{I1}^2 - \omega_{I2}^2)(n-1)\left(\frac{1}{pT_{1p}}\right)_{ML}\right] \quad (9)$$

where the subscripts 1 and 2 represent relaxation rate values measured at frequencies 1 and 2. An analogous relationship can be obtained in terms of frequencies 2 and 3. The two equations can be written as an equality, and the equation can be solved in terms of n (eq 10).

$$n = 1 + \left\{\omega_{I1}^2\left[\left(\frac{1}{pT_{1p}}\right)_1\left(\frac{1}{pT_{1p}}\right)_3 - \left(\frac{1}{pT_{1p}}\right)_1\left(\frac{1}{pT_{1p}}\right)_2\right] + \omega_{I2}^2\left[\left(\frac{1}{pT_{1p}}\right)_1\left(\frac{1}{pT_{1p}}\right)_2 - \left(\frac{1}{pT_{1p}}\right)_2\left(\frac{1}{pT_{1p}}\right)_3\right] + \omega_{I3}^2\left[\left(\frac{1}{pT_{1p}}\right)_2\left(\frac{1}{pT_{1p}}\right)_3 - \left(\frac{1}{pT_{1p}}\right)_1\left(\frac{1}{pT_{1p}}\right)_3\right]\right\} \Big/ \left\{\left(\frac{1}{pT_{1p}}\right)_{ML}\left[(\omega_{I2}^2 - \omega_{I3}^2)\left[\left(\frac{1}{pT_{1p}}\right)_2 - \left(\frac{1}{pT_{1p}}\right)_3\right] + (\omega_{I2}^2 - \omega_{I3}^2)\left[\left(\frac{1}{pT_{1p}}\right)_2 - \left(\frac{1}{pT_{1p}}\right)_1\right]\right]\right\} \quad (10)$$

Thus the distribution of Mn^{2+} between the binary Mn–ligand and the enzyme–Mn–ligand(s) complexes can be determined by a frequency dependence of $1/pT_{1p}$. The value of n is related to the value of $(1/pT_{1p})_{obsd}$ at each frequency, the frequency of observation, ω_I, and the value $1/pT_{1p}$ for the binary complex $[(1/pT_{1p})_{ML}]$.

The frequency dependence of the ^{31}P relaxation rates was measured for both the ternary E–Mn–P_i and quaternary E–Mn–F–P_i complexes, and the distribution of Mn^{2+} in the enzymatic and nonenzymatic complexes was calculated. The distribution of Mn^{2+}, when ^{19}F relaxation rates were measured in the quaternary complex, was based on calculations performed from ^{31}P measurements since the experiments were performed under nearly identical conditions.

Calculation of τ_c and of r. From the observed frequency dependence of the $1/pT_{1p}$ for ^{31}P, it is clear that the relaxation rate is in the fast exchange region and $1/pT_{1p} = 1/T_{1M}$. From the frequency dependence of $1/T_{1M}$, the value of τ_c can be estimated by using eq 6. With values for τ_c, the electron-nuclear distance, r, can thus be calculated for Mn–^{31}P and Mn–^{19}F in the respective ternary and quaternary complexes.

Chemical Exchange Rates. The Swift–Connick equations (eq 5a,b) describe the effect of chemical exchange ($1/\tau_M$) on relaxation. The normalized relaxation rates can thus yield values for the exchange rate ($1/\tau_M$) or a limit to the exchange rate $1/\tau_M > 1/pT_{2p}$ of the ligand under investigation. Since $T_{2M} \leq T_{1M}$, it is possible that although $1/pT_{1p}$ is in fast exchange, $1/pT_{2p}$ may be in the slow exchange region, thus yielding kinetic information concerning complex formation. Two criteria are obvious. If $1/pT_{np}$ is in slow exchange, the value for the relaxation rate would be frequency independent. If $1/pT_{np}$ is dominated by τ_M, then Arrhenius behavior is expected when a temperature dependence of $1/pT_{np}$ is measured. Exchange rates and their energy barriers can be

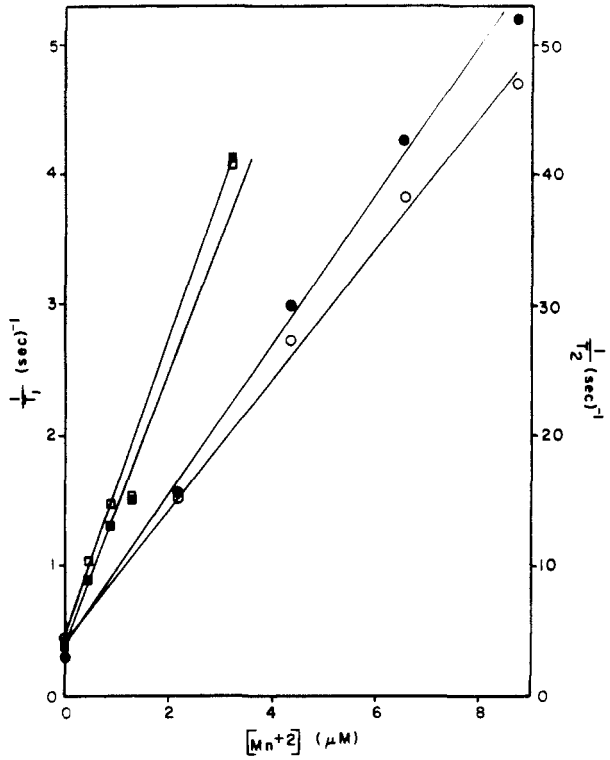

FIGURE 1: Effect of Mn^{2+} on the $1/T_1$ and $1/T_2$ values of F^-. The values of $1/T_1$ and $1/T_2$ for F^-, measured at 0.1 and 0.5 M KF are shown as a function of Mn^{2+}. The experiments performed at 0.1 M KF are designated by boxes, and those performed at 0.5 M KF are designated by circles. The opened boxes or circles designate $1/T_1$ values while the closed boxes or circles designate $1/T_2$ values.

estimated from a measurement of $1/pT_{2p}$ as a function of temperature.

The binding of Mn^{2+} to the enzyme, to the ligands F^- and P_i, and to enzyme–ligand complexes was measured by EPR by using the methods of Cohn & Townsend (1954). Spectra of Mn^{2+} were obtained on a Varian V4500 EPR spectrometer at room temperature.

Results

Binary Mn–F Complex. The effect of Mn^{2+} on T_1 and T_2 of the ^{19}F nucleus of the fluoride anion was measured. The relaxation parameters and K_d of the binary Mn–F complex were determined by high-resolution ^{19}F experiments. When eq 2 was solved simultaneously at two concentrations of F^-, both K_d and $1/pT_{np}$ (n = 1 or 2) were obtained. Both 0.1 and 0.5 M KF solutions were titrated with Mn^{2+}. The $1/T_1$ and $1/T_2$ values were measured at 94.1 MHz for each concentration of Mn^{2+}. The results are plotted in Figure 1 as $1/T_1$ and $1/T_2$ vs. [Mn^{2+}]. The data yield a linear response with slope m. When m and [F^-] as measured values are used, eq 2 yields both $1/pT_{np}$ and K_d when solved simultaneously at the two concentrations of F^-. The $1/T_1$ data result in K_d = 0.29 M and $1/pT_{1p} = 4.48 \times 10^5$ s^{-1}. The data for $1/T_2$ yield K_d = 0.32 M and $1/pT_{2p} = 4.58 \times 10^6$ s^{-1}.

An independent determination of K_d for the Mn–F complex was made by using EPR spectroscopy (data not shown). The value obtained by an EPR titration, $K_d = 0.30 \pm 0.03$ M, is in excellent agreement with the NMR ^{19}F relaxation rate results shown above. This value is somewhat lower than that previously reported for Mn–F, $K_d = 0.4 \pm 0.14$ M (Mildvan et al., 1967), which was determined under somewhat different conditions.

Relaxation Parameters for ^{19}F in the Ternary Enolase–Mn–F Complex. The PRR titration data (Maurer & Nowak, 1981) suggested that F^- binds directly to the bound Mn^{2+} and displaces one of the two bound water molecules. The interaction of F^- with enolase–Mn was studied directly by a measure of the effects of bound Mn^{2+} on the relaxation rates of ^{19}F at 94.1 MHz. The experiment was designed to obtain data useful in calculating the normalized relaxation rates ($1/pT_{1p}$ and $1/pT_{2p}$) of ^{19}F in the ternary, E–Mn–F complex. To this end, small amounts of $MnCl_2$ were titrated into a buffered solution of enolase containing KF. The $1/T_1$ and $1/T_2$ values of ^{19}F at 94.1 MHz and at 30 °C were measured at each concentration of Mn^{2+}. The values of $1/T_1$ and $1/T_2$ increase linearly with increasing concentrations of Mn^{2+} as shown in Figure 2. The effect of Mn^{2+} on the ^{19}F relaxation rates must be resolved into two components, the contribution from enzyme-bound Mn^{2+}, which exerts its effect on F^- in the EMF complex, and the contribution from non-enzyme-bound Mn^{2+}. The enzyme-bound Mn^{2+} can be readily calculated from the known dissociation constants of the enolase–Mn complex (K_s = 10 μM) measured under experimental conditions (Nowak et al., 1973; P. J. Maurer and T. Nowak, unpublished observations) and the total concentrations of enolase and Mn^{2+} used in the experiment. With 121 μM enzyme and 0–6.4 μM Mn^{2+}, approximately 92% of the Mn^{2+} is enzyme bound. The concentration of F^- used in the experiment does not significantly alter this distribution. This enzyme-bound Mn^{2+} contributes to the slope of the plots in Figure 2 through the second term of eq 3. The remaining 8% of the Mn^{2+} contributes to the slope through the first term of eq 3. When eq 3 and the data obtained for the binary complex are used, the normalized paramagnetic effect on the relaxation rates, $1/pT_{1p}$ and $1/pT_{2p}$, can be calculated for ^{19}F in the ternary EMF complex (Table II). The relaxation rate values calculated from Figure 2 are given in Table I.

Clearly $1/pT_{1p}$ of ^{19}F in the EMF complex is greater than $1/pT_{1p}$ of ^{19}F in the MF complex, indicating the enzyme causes an enhancement (greater than unity) in the paramagnetic

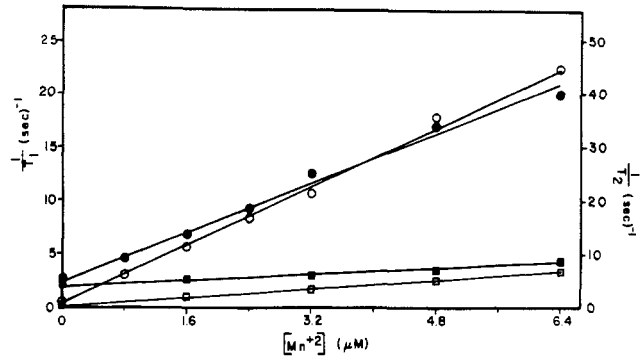

FIGURE 2: Effect of Mn^{2+} on the ^{19}F relaxation rates of KF in the presence of enolase. The plot of $1/T_1$ and $1/T_2$ of ^{19}F vs. [Mn^{2+}] summarizes the results obtained in the presence of 121 μM enolase which contains 50 mM KCl and 50 mM Tris-HCl, pH 7.5 (O). An analogous experiment which also included 2 mM P_i is designated by boxes. The open circles or boxes represent $1/T_1$ values, and the closed circles or boxes represent $1/T_2$ values.

Table I: Normalized Relaxation Rates of the F^- and P_i Ligands in the Enolase–Mn Complexes

nucleus	complex	$1/pT_{1p}$ (s^{-1})	$1/pT_{2p}$ (s^{-1})
^{19}F[a]	E–Mn–F	(3.49 ± 0.37) × 10^5	(5.5 ± 1.1) × 10^5
	E–Mn–F–P_i	(4.46 ± 0.39) × 10^4	(5.2 ± 0.5) × 10^4
^{31}P[b]	E–Mn–P_i	(3.56 ± 0.21) × 10^3	(32.5 ± 2.6) × 10^3
	E–Mn–F–P_i	(1.13 ± 0.05) × 10^3	(13.9 ± 1.6) × 10^3

[a] Measured at 94.1 MHz at 30 °C. [b] Measured at 40.5 MHz at 30 °C.

effect on the relaxation rate of ^{19}F as F^-. The values for $1/pT_{1p}$ and $1/pT_{2p}$ for the ternary (E–Mn–F) complex are nearly equal.

Relaxation Parameters for ^{19}F in the Quaternary Enolase–Mn–P_i–F Complex. For an assessment of the effect of P_i on the interaction between enzyme-bound Mn^{2+} and F^-, the values of $1/T_1$ and $1/T_2$ of F^- were determined as a function of the concentration of Mn^{2+} in the presence of enolase and P_i. The concentration of P_i used (2–16 mM) is sufficient to effectively saturate the E–M complex without significantly competing with the enzyme for Mn^{2+} binding. This is rigorously demonstrated in the following section of ^{31}P relaxation parameters. The slope of the plot of the resulting data (Figure 2) was used in eq 3 to determine $1/pT_{1p}$ and $1/pT_{2p}$ for ^{19}F in the E–Mn–P_i–F quaternary complex. The addition of P_i to the solution containing enolase, Mn^{2+}, and F^- tightens the binding of Mn^{2+} to the enzyme so that the first term in eq 3 is approximately equal to zero (see below). That is, $(f)_b$, the fraction of the Mn^{2+} which is enzyme bound, is essentially 1, and $(f)_f$, the fraction of Mn^{2+} which is not bound to the enzyme, is negligible. Also, since the concentration of F^- used in the experiment is much greater than the dissociation constant of F^- from the quaternary complex, K_d may be dropped from eq 3, yielding the relationship $m = (1/pT_{np})/[F^-]$ (n = 1 or 2). Calculation of $1/pT_{1p}$ and $1/pT_{2p}$ yields the values given in Table I.

Diamagnetic efects on the relaxation rates of ^{19}F, determined by the addition of Mg^{2+} to the solutions of enzyme and F^- (with or without P_i), are not observable even at Mg^{2+} levels which are 10 times higher than the levels of Mn^{2+} used. Thus, the increase in relaxation rates of ^{19}F by Mn^{2+} is a paramagnetic effect and not an effect modulated by a metal ion induced protein conformational change or other effects. The enolase–Mg complex is even more potently inhibited by fluoride and P_i than is the Mn^{2+} enzyme (Wang & Himoe, 1974).

Competition between F^- and PEP/2-PGA for the Enolase Binding Site. It has previously been demonstrated that in the presence of P_i, fluoride is a linear competitive inhibitor of Mg^{2+}-activated rabbit muscle enolase (Wang & Himoe, 1974). In order to show whether F^- competes with substrate (PEP $\rightleftharpoons$ 2-PGA) for the catalytic site of the yeast enzyme, the relaxation rates of ^{19}F in the E–Mn–F complex were measured as a function of substrate concentration. A solution containing 121 μM enolase sites, 0.1 M KF, and 6.4 μM $MnCl_2$ was titrated with D(+)-2-PGA (0–75.2 μM), and $1/T_1$ and $1/T_2$ were measured at each concentration of substrate. The $1/T_1$ and $1/T_2$ of ^{19}F decrease with increasing concentrations of substrate. Moreover, the data could be fit with a theoretical curve based on simple competition between F^- and substrate assuming a K_d for F^- of 0.6 M and a K_d for substrate of 0.11 mM. These results demonstrate that F^- does indeed compete with PEP and/or 2-PGA for the active site of Mn^{2+} yeast enolase.

Michaelis constants and dissociation constants of 2-PGA and PEP with Mn–enolase vary widely among reports in the literature (i.e., Hanlon & Westhead, 1969; Nowak et al., 1973; Wang & Himoe, 1974), but the apparent value of 0.11 mM determined in this paper is within the range of values reported. It may be that 0.11 mM is a fortuitously high value since this experiment specifically measures effects of the Mn–enolase complex amidst an overwhelming concentration of apoenzyme which may bind significant amounts of the added substrate. The experimental conditions utilized here were not identical with those used in an enzyme assay. The binding of substrate to apoenolase under the conditions of our experiment has not been adequately investigated. It is also not clear if PGA or if both substrates will actually displace F^-.

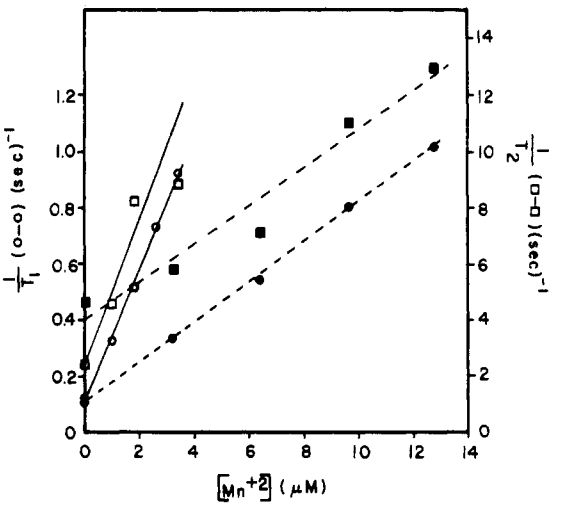

FIGURE 3: Effect of Mn^{2+} on $1/T_1$ and $1/T_2$ of ^{32}P. The results of a titration of $1/T_1$ and $1/T_2$ of ^{32}P in the ternary and the quaternary complexes containing P_i are shown. The experiments were performed as described in the text with varying $[Mn^{2+}]$ as indicated. The circles represent $1/T_1$ values and the squares $1/T_2$ values. The values for the ternary complex are represented by opened circles and squares, and the values for the quaternary complex are represented by filled circles and squares and by broken lines.

Relaxation Rate Studies of ^{31}P. Experiments were performed to determine the effect of enolase-bound Mn^{2+} on the relaxation rates of ^{31}P of P_i in order to clarify the role of P_i in enolase inhibition. P_i is both a competitive inhibitor of enolase and a "coinhibitor" in the case of the strong inhibition by P_i in the presence of F^- (Wang & Himoe, 1974). So that this problem could be studied, a solution of enzyme and P_i was titrated with $MnCl_2$, and the relaxation rates of ^{31}P at 40.5 MHz and 30 °C were determined at each concentration of Mn^{2+}. These experiments are analogous to those involving ^{19}F as previously described. The results are plotted in Figure 3 as $1/T_1$ and $1/T_2$ vs. $[Mn^{2+}]$. The Mn^{2+} produces a significant increase in $1/T_1$ and in $1/T_2$. The slope of the plot (m) from Figure 3 is used (as in the case of ^{19}F relaxation) to determine the normalized relaxation rates for ^{31}P in the E–Mn–P_i complex by means of eq 3. The calculated value is given in Table I. The possibility of a significant contribution to the observed rates from the nonenzymatic Mn–P_i complex was ruled out by the frequency dependence of $1/pT_{1p}$ (see below). So that the Mn^{2+}–^{31}P interaction in the quaternary E–Mn–P_i–F complex could be studied, the measurement of $1/T_1$ of ^{31}P as a function of $[Mn^{2+}]$ was repeated in the presence of KF. A plot of $1/T_1$ and $1/T_2$ vs. Mn^{2+} concentration demonstrates a more shallow slope than that measured for the ternary complex. The data is also plotted in Figure 3. The slope was used in eq 3 to determine the normalized paramagnetic relaxation rates of ^{31}P in the quaternary E–Mn–P_i–F complex. The normalized values are summarized in Table I.

Temperature Effects of the Parmagnetic Relaxation Rates of ^{19}F and ^{31}P in Enolase–Mn Complexes. As previously described (Mildvan & Cohn, 1970), the observed paramagnetic contribution to the relaxation rates of nuclei in enzyme complexes may be affected by two different processes: (a) chemical exchange of the nucleus from the paramagnetic site with a residence time, τ_M, and (b) the inherent relaxation rates of the nucleus at the paramagnetic site which have time constants T_{1M} and T_{2M}. The slower of these two processes will dominate

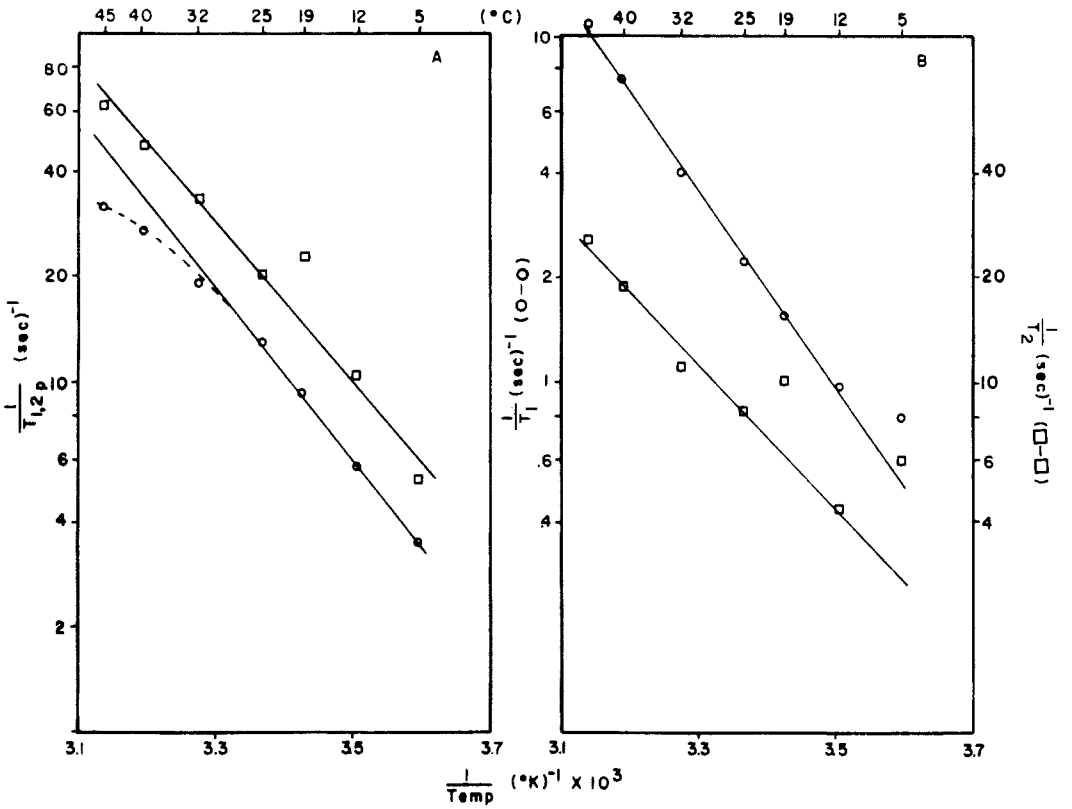

FIGURE 4: Temperature dependence of the ^{19}F relaxation rates of the ternary (E–Mn–F) and the quaternary (E–Mn–F–P) complexes. The data in (A) show the temperature dependence of the paramagnetic effect of bound Mn^{2+} on the $1/T_1$ (O) and the $1/T_2$ (□) values in the ternary complex. The sample, in 0.6 mL, contained 0.1 M KF, 121 μM enolase, 6.4 μM $MnCl_2$ in 50 mM Tris-HCl, pH 7.5, and 50 mM KCl. The paramagnetic effect was calculated by subtraction of a diamagnetic control measured under identical conditions as described under Materials and Methods. The dotted line, designated for $1/T_{1p}$ at the higher temperatures, is suggestive of the onset of the rapid exchange region. This suggestion and the resulting calculations are outlined under Discussion. The results in (B) show the temperature dependence of $1/T_1$ (O) and $1/T_2$ (□) measured for ^{19}F in the quaternary in (E–Mn–F–P_i) complex. The sample was identical with that used in (A) with the inclusion of 2 mM P_i.

the observed normalized rate $1/pT_{1p}$ and $1/pT_{2p}$ as described mathematically by eq 5. The effect of temperature on the observed values of $1/pT_{1p}$ and $1/pT_{2p}$ can be used to determine the dominant (slowest) process (Luz & Meiboom, 1964).

The $1/T_1$ and $1/T_2$ relaxation rates of ^{19}F and ^{31}P in their respective ternary and quaternary complexes of enolase–Mn were measured as a function of temperature over the range 0–45 °C. The upper temperature is limited by the thermal stability of enolase. The experiments were performed in a manner analogous to those previously described but at a fixed concentration of Mn^{2+}. Conditions of each experiment were chosen to obtain the optimal signal-to-noise and to have the maximal fraction of Mn^{2+} in the enzyme complex. Solutions which were identical except for the lack of Mn^{2+} served as a diamagnetic control. Relaxation rates of the respective ternary and quaternary enzyme–Mn^{2+} complexes were measured for ^{19}F and for ^{31}P at each temperature. Differences in relaxation rates between the Mn^{2+} containing complex and the diamagnetic control gave values for the paramagnetic contribution to the relaxation rates.

The results of the temperature study of the ^{19}F and ^{31}P relaxation rates of the ternary and quaternary complexes are plotted in Arrhenius fashion in Figures 4 and 5. The negative slopes are characteristic of slow chemical exchange. The similar values of $1/pT_{1p}$ and $1/pT_{2p}$ for ^{19}F in the ternary and quaternary complexes support this conclusion. In these complexes apparently τ_M dominates the ^{19}F relaxation process. In the ternary complex, the data suggest that at the highest temperature observed, relaxation is just beginning to depart from slow exchange. No such indication is suggested for the quaternary complex (Figure 4).

Table II: Kinetic and Relaxation Rate Parameters of the F^- and the P_i Ligands in the Enolase-Mn Complexes

nucleus	complex	$1/T_{1M}$ (s^{-1})	$1/\tau_M$ (s^{-1})	r (Å)
^{19}F	E-Mn-F	$>2.6 \times 10^6$	3.5×10^6 [a]	<2.2
	E-Mn-F-P_i	$>4.5 \times 10^4$	5.2×10^4 [b]	<4.4
^{31}P	E-Mn-P_i	3.6×10^3	3.3×10^4 [c]	6.48 ± 0.20
	E-Mn-F-P_i	1.1×10^3	1.4×10^4 [d]	7.66 ± 0.21

[a] E_{act} = 11.6 kcal/mol; $k_{on} = 5.6 \times 10^6$ M^{-1} s^{-1}. [b] E_{act} = 12.2 kcal/mol; $k_{on} = 2 \times 10^7$ M^{-1} s^{-1}. [c] E_{act} = 6.8 kcal/mol; $k_{on} = 2.75 \times 10^7$ M^{-1} s^{-1}. [d] E_{act} = 16.6 kcal/mol; $k_{on} = 7.4 \times 10^8$ M^{-1} s^{-1}.

The data from ^{31}P studies suggest rapid exchange for longitudinal relaxation, although apparent Arrhenius behavior is observed. First, the values for $1/pT_{2p}$ for ^{31}P are an order of magnitude greater than those for $1/pT_{1p}$ both in the ternary (EMP) and quaternary (EMFP) complexes. If $1/pT_{1p}$ was dominated by chemical exchange, then $1/pT_{1p}$ would equal $1/pT_{2p}$ (see eq 5a and 5b). Second, the values for $1/pT_{1p}$ for both complexes demonstrate a strong frequency dependence (see below). Only relaxation, not chemical exchange, can exhibit a frequency dependence. Therefore, the values for $1/pT_{1p}$ must equal $1/T_{1M}$ for ^{31}P in both the ternary and quaternary complexes. A summary of the data obtained from these experiments is given in Table II.

Frequency Dependence of $1/pT_{1p}$ of ^{31}P in Ternary E–Mn–P_i and Quaternary E–Mn–P_i–F Complexes. The frequency dependence of $1/pT_{1p}$ of ^{31}P in the enolase–Mn complexes containing P_i was studied for three reasons. First, the results will demonstrate whether the observed rates are dom-

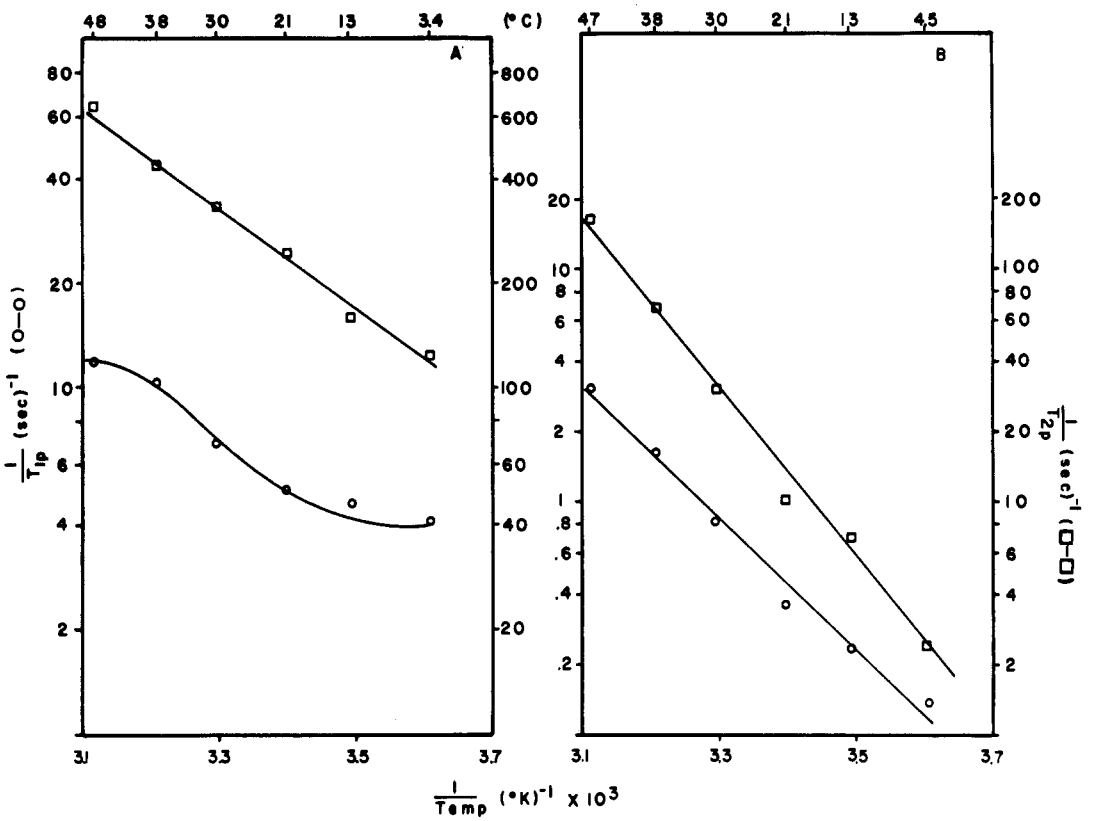

FIGURE 5: Temperature dependence of the paramagnetic effects on $1/T_1$ and $1/T_2$ of ^{31}P in the ternary and quaternary complexes. In (A), the paramagnetic effects on ^{31}P of P_i in the ternary (E–Mn–P_i) complex are shown. The results for $1/T_{1p}$ (O) and $1/T_{2p}$ (□) are plotted vs. 1/temp. The experiment, performed in a 2 mL volume and measured at 40.5 MHz, contained 50 mM Tris-HCl, pH 7.5, 50 mM KCl, 116 μM enzyme, 0.1 M P_i, and 50 μM $MnCl_2$ in D_2O. The experiments in (B) were performed for the quaternary (E–Mn–F–P_i) complex under identical conditions described for (A) with the inclusion of 25 mM KF. The absolute values for $1/T_{1p}$ are given on the left ordinate while the values for $1/T_{2p}$ are given on the right ordinate for both (A) and (B).

inated by chemical exchange or by relaxation. Second, from the values of $1/pT_{1p}$ at three frequencies, the distribution of Mn^{2+} between enzyme-bound and non-enzyme-bound forms can be calculated as described under Material and Methods. Third, the frequency dependence of the relaxation rates can be used to calculate the value of the correlation time for the Mn^{2+}–P_i interactions. The determination of $1/pT_{1p}$ for ^{31}P in the EMP and EMFP complexes by titration of enzyme solutions with Mn^{2+} was performed at 60.7 and 145.8 MHz under conditions (concentrations and temperature) identical with those described at 40.5 MHz. The data are plotted in Figure 6 as $1/T_1$ vs. $[Mn^{2+}]$. As before, the slope (m) was used to calculate $1/pT_{1p}$. It is apparent that a strong frequency dependence is observed. The values for $1/pT_{1p}$ decrease substantially as the frequency increases. The results eliminate the possibility of slow exchange and indicate that $1/pT_{1p}$ is a measure of $1/T_{1M}$ and not $1/\tau_M$. It is also immediately apparent that a large fraction of the total Mn^{2+} is bound to the enzyme (this fraction is calculated below) since the interaction of P_i with unbound Mn^{2+} would not be expected to show a significant frequency dependence.

Distribution Calculations. The value of n, the fraction of the Mn^{2+} which is bound to the enzyme (see eq 4) under the experimental conditions ($[Mn^{2+}]$ = 0–6.4 μM), can be determined from the results of the frequency dependence studies above and from $1/pT_{1p}$ of the simple Mn–P_i complex (12 000 s^{-1}; Nowak, 1978) which is frequency independent over the region of observation. From the data in Figure 6 and the use of eq 10, n is calculated to be 1.01 for the ternary EMP complex and 1.03 for the quaternary EMFP complex. Thus, essentially all of the Mn^{2+} is enzyme bound in the experiments where P_i is present. Only when P_i is absent, in the case of the

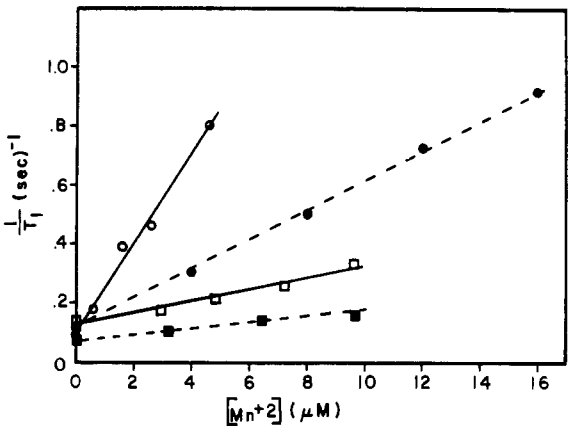

FIGURE 6: Effect of Mn^{2+} on the $1/T_1$ values of ^{31}P of P_i for the ternary and quaternary complexes at 60.7 and 145 MHz. The experiments were performed under identical conditions to those performed in Figure 3. The circles represent data obtained at 60.7 MHz, and the squares represent data obtained at 145 MHz. The opened circles and squares represent data obtained for the ternary complexes while the solid circles and squares represent data obtained for the quaternary complex.

ternary EMF complex, would non-enzyme-bound Mn^{2+} be expected to contribute to the relaxation rate of the observed nucleus, ^{19}F via the binary Mn–F complex. Even in that case, however, the nonenzymatic contribution is accounted for by using both terms of eq 3.

Calculation of τ_c from the Frequency Dependence of $1/pT_{1p}$ of ^{31}P. So that the paramagnetic relaxation rate ($1/T_{1M}$) of a nucleus within a paramagnetic complex can be related to the distance (r) between the paramagnetic spin and the nucleus, using the Solomon–Bloembergen equation (eq 6), a value for the correlation time function [$f(\tau_c)$] for the relaxation

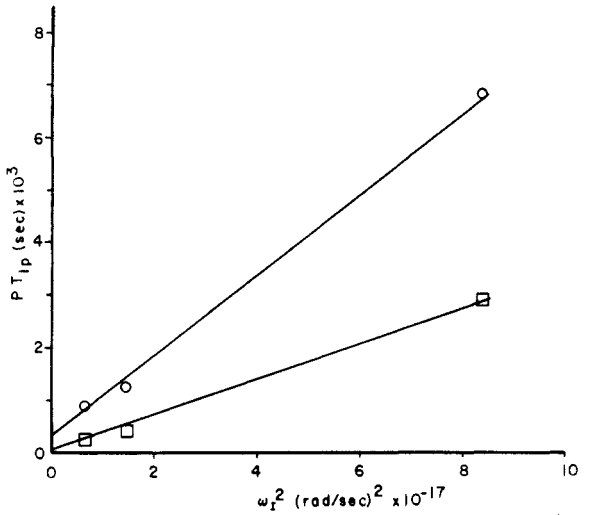

FIGURE 7: Frequency dependence of ^{31}P relaxation rates of P_i in the ternary and quaternary enolase complexes. The normalized paramagnetic effects on the longitudinal relaxation times of P_i were calculated from data shown in Figures 3 and 6. The results are plotted as a function of frequency squared. The results obtained for the ternary E–Mn–P_i complex are designated by boxes, and the results for the quaternary E–Mn–F–P_i complex are designated by circles. The experiments were performed under identical conditions at each frequency.

process is required. As expressed in eq 7, the correlation time function is the sum of two terms. However, in the case of Mn^{2+} complexes, the first term in eq 7 is much larger than the second term, and a good approximation is obtained by ignoring the second term altogether. Thus, when eq 6 is rearranged and the first term of eq 7 is used to express $f(\tau_c)$, the following expression is obtained:

$$T_{1M} = \left[\left(\frac{r}{c}\right)^6\left(\frac{\tau_c}{3}\right)\right]\omega_I^2 + \left[\left(\frac{r}{c}\right)^6\left(\frac{1}{3\tau_c}\right)\right] \quad (11)$$

By plotting T_{1M} as a function of ω_I^2, one obtains a slope of $[(r/c)^6(\tau_c/3)]$ and a y intercept of $[(r/c)^6(1/3\tau_c)]$. When the slope is divided by the y intercept, τ_c^2 is obtained. Thus, the frequency dependence of $1/T_{1M}$ serves in the calculation of τ_c. In Figure 7, T_{1M} of ^{31}P is plotted as a function of ω_I^2 for both the ternary and quaternary complexes. The plot is linear and suggests that τ_c is approximately frequency independent over the range measured. By the method discussed above, τ_c is calculated to be 9.01×10^{-9} s for the ternary EMP complex and 5.83×10^{-9} s for the quaternary complex. This calculation is made by assuming no frequency dependence of τ_c. The value of τ_c is approximately the value expected for τ_s of Mn^{2+} [τ_s(free Mn^{2+}) = 3×10^{-9} s] and agrees with other values estimated for enolase–Mn complexes (Nowak et al., 1973). Calculations of τ_c from the ratio of $1/T_{1M}$ at any two frequencies allow estimates of extreme values of τ_c for the ternary and the quaternary complexes. These calculations lead to values of $\tau_c = (6.4 \times 2.6) \times 10^{-9}$ s and $\tau_c = (5.4 \pm 2.5) \times 10^{-9}$ s, respectively.

Calculations of Interatomic Distances: Mn–^{31}P and Mn–^{19}F in the Inhibitory Enolase Complexes. The interatomic distances of Mn–^{31}P and Mn–^{19}F in the inhibitory enolase complexes are important parameters in describing the structures of these complexes. The values may be calculated from nuclear relaxation data via the Solomon–Bloembergen equation (eq 6). Solving eq 6 for r yields

$$r = C[T_{1M}f(\tau_c)]^{1/6} \quad (12)$$

When seconds are used as units of τ_c and T_{1M} and angstrom units for r, the constant C has the value 601 for the Mn–^{31}P interaction and 796 for the Mn–^{19}F interaction (Mildvan & Engle, 1972).

From the values of τ_c calculated above, the following correlation time function ($f(\tau_c)$] values are obtained for a frequency of 40.5 MHz: $f(\tau_c)_{40.5MHz} = (5.26 \pm 0.78) \times 10^{-9}$ for EMP and $f(\tau_c)_{40.5MHz} = (5.60 \pm 0.45) \times 10^{-9}$ for EMFP.

Using these values of $f(\tau_c)$ in the calculation of interatomic Mn–^{31}P distances for the enzyme complexes leads to $r = 6.5 \pm 0.2$ Å for EMP and $r = 7.7 \pm 0.2$ Å for EMFP. These values of r preclude the possibility of direct coordination between Mn and P_i in either complex. Direct coordination would require a value of $r \leq 3.7$ Å.

Since the relaxation rates of ^{19}F were not studied as a function of frequency, a reasonable value of $f(\tau_c)$ must be estimated. The value of τ_c is dominated by τ_s, the electron relaxation time, and possibly a contribution by τ_r, the rotational correlation time. Both of these values would be expected to be very nearly constant from one enolase complex to the next. Furthermore, the values estimated for τ_c for enolase–Mn complexes, described here and elsewhere (Nowak et al., 1973), yield nearly identical values. Therefore, it is reasonable to assume that τ_c for the E–Mn–^{19}F interaction is equal to τ_c for the E–Mn–^{31}P interactions. Thus, the average value of τ_c calculated for ^{31}P in the ternary and quaternary complexes are used in the calculation of Mn–^{19}F distance limits in the enzyme complexes. The values for $1/pT_{1p}$ of ^{19}F are dominated by chemical exchange ($1/pT_{1p} = 1/\tau_{M_1}$). Therefore, these values are lower limits to the values of $1/T_{1M}$ for ^{19}F in the ternary and quaternary complexes and yield upper limits to the values of r which are calculated.

With this in mind, evaluation of r gives $r < 2.3$ Å for E–Mn–^{19}F and $r < 4.3$ Å for E–Mn–^{19}F–P_i. In the ternary complex, F^- must be in the first coordination sphere of Mn^{2+}. Crystallographic data on MnF_2 crystals yield a Mn–F distance of 2.12 Å (Griffel & Stout, 1950), and no known chemical species could intervene between Mn and F^- with an increased separation of only 0.2 Å. In the quaternary complex, there is no evidence that the Mn–^{19}F distance is any greater than that in the ternary complex; the increase in the upper limit value of r can be attributed entirely to an increased residence time of F^- in the complex. Indeed, it is certain that the residence time is longer in the quaternary complex since $1/pT_{1p}$ is essentially a measure of $1/\tau_M$ in the case of the slow exchange limit. Furthermore, the K_d value for F^- decreases. Lacking further evidence to the contrary, the simplest model consistent with the data leaves the Mn–^{19}F distance unaltered by the binding of P_i. Additional relaxation studies at higher fields may resolve this ambiguity.

Exchange Rates (k_{off}) and Activation Parameters for Ligand Dissociation. From the temperature dependence of the paramagnetic effect on the relaxation rates of ^{19}F in the E–Mn–F and E–Mn–P_i–F complexes and from the similarity in values of $1/pT_{1p}$ and $1/pT_{2p}$ for these complexes, it is apparent that the relaxation rates measured are a reflection of ligand exchange rates ($1/\tau_M$) rather than relaxation rates ($1/T_{1M}$ or $1/T_{2M}$). Thus, for ^{19}F, $1/pT_{1p} \approx 1/pT_{2p} = k_{off}$. At 30 °C, k_{off} for F^- is 2.6×10^6 s^{-1} and 4.5×10^4 s^{-1} from the ternary and quaternary complexes, respectively. Also, assuming the simplest model for Mn–ligand formation with F^-, $k_{on} = k_{off}/K_d$. Therefore k_{on} can be calculated. At 30 °C, k_{on} for F^- is 5.6×10^6 M^{-1} s^{-1} and 19×10^6 M^{-1} s^{-1} for the ternary and quaternary complexes, respectively. From the temperature dependence of k_{off}, the activation parameters for dissociation ($\Delta H^\ddagger$, $\Delta S^\ddagger$) can be calculated for F^-. For the

E–Mn–F complex, $\Delta H^{\ddagger}$ = 11.0 kcal/mol, $\Delta S^{\ddagger}$ = 7.7 eu, and $\Delta G^{\ddagger}$ = 8.7 kcal/mol. For the E–Mn–F–P_i complex, $\Delta H^{\ddagger}$ = 11.6 kcal/mol, $\Delta S^{\ddagger}$ = 1.3 eu, and $\Delta G^{\ddagger}$ = 11.2 kcal/mol. The decrease in k_{off} for F^- from the quaternary complex is primarily a result of an entropy contribution.

An analogous analysis of the $1/pT_{2p}$ data for ^{31}P in the ternary and quaternary complexes was performed. The $1/T_{2p}$ data gave Arrhenius behavior, and $1/pT_{2p}$ for the ternary and quaternary complexes showed no significant frequency dependence at 40.5 and 60.7 MHz, suggesting $1/pT_{2p} = 1/\tau_M$ for the P_i ligand in both complexes. The decrease in k_{off} of P_i upon formation of the quaternary complex is the result of a large increase in the energy of activation (+10 kcal/mol), suggesting a more highly complexed ligand. This is due to both a sizeable enthalpy change ($\Delta H^{\ddagger}$ = 6.2 vs. 16.0 kcal/mol) and an entropy effect ($\Delta S^{\ddagger}$ = −17.5 eu vs. 13.7 eu) for the ternary complex vs. the quaternary complex. A summary of the kinetic and thermodynamic data is outlined in Table II.

Dissociation Constants for Mn^{2+} from the Inhibitory Complexes. Under experimental conditions where $1/pT_{1p}$ of ^{31}P was determined in the ternary E–Mn–P_i complex (16 mM P_i, 0–6.4 μM Mn^{2+}), all of the Mn^{2+} was shown to be enzyme bound (see above). When the concentration of P_i was increased to 0.1 M, however, competition between enzyme and P_i becomes significant. The distribution of Mn^{2+} between E–Mn–P_i and Mn–P_i complexes can be determined from the observed $1/pT_{1p}$ since $(1/pT_{1p})_{obsd} = n(1/pT_{1p})_{E\text{-}MnP_i} + (1 - n)(1/pT_{1p})_{Mn\text{-}P_i}$. The value of n is the fraction of Mn^{2+} which is enzyme bound. The value for $(1/pT_{1p})_{Mn\text{-}P_i}$ is 12×10^3 s^{-1} (Nowak, 1978), and the value for $(1/pT_{1p})_{E\text{-}Mn\text{-}P_i}$ was determined as 3.96×10^3 s^{-1} as described (Table I). The value of $(1/pT_{1p})_{obsd}$, measured at 0.1 M P_i (8.95×10^3 s^{-1}) yields a value of n = 0.379. The dissociation constant

$$K_{d(E\text{-}Mn\text{-}P)} = \frac{[EP]\,[Mn]}{[EMnP]} \qquad (13)$$

and since $K_{d(Mn\text{-}P_i)}$ = 1.2 mM, therefore

$$\frac{K_{d(Mn\text{-}P_i)}}{K_{d(E\text{-}Mn\text{-}P_i)}} = \frac{[P]\,[EMnP]}{[EP]\,[MnP]}$$

Rearrangement yields the relationship

$$K_{d(E\text{-}Mn\text{-}P)} = \frac{K_{d(Mn\text{-}P_i)}\,[Mn\text{-}P]\,[EP]}{[EMnP]\,[P]} \qquad (14)$$

Since $[Mn\text{-}P] = (1 - n)\,[Mn^{2+}]_t$, $[EP] \approx [E]_t$, $[P] \approx [P]_t$, and $[EMnP] = n[Mn^{2+}]_t$, $K_{d(E\text{-}Mn\text{-}P)}$ can be evaluated. The value for $K_d = 2.9 \times 10^{-6}$ M.

An analogous evaluation of K_d for Mn^{2+} from the quaternary E–Mn–F–P_i complex can also be performed. The value of $(1/pT_{1p})_{obsd} = 2.61 \times 10^3$ s^{-1} was obtained at 0.1 M P_i. The value for $(1/pT_{1p})_{E\text{-}Mn\text{-}F\text{-}P} = 1.13 \times 10^3$ s^{-1} (Table I) yields an evaluation for n = 0.863. The K_d value, calculated from these results, yields $K_{d(E\text{-}Mn\text{-}F\text{-}P_i)} = 0.29 \times 10^{-6}$ M. The addition of F^- increases the binding of Mn^{2+} by an order of magnitude compared to the binding of Mn^{2+} to the ternary E–Mn–P_i complex. Thus a complex set of interactions are observed whereby each ligand not only tightens the binding of the complementary ligand but also increases the binding of the metal ion itself.

Discussion

Fluoride effects in biochemical systems have been observed both in vivo and in vitro. Although several metabolic pathways such as fatty acid synthesis and the pentose phosphate pathway have been shown to be inhibited by F^-, glycolysis–gluconeogenesis is the most well-documented pathway which is inhibited. While adenylate cyclase is an example of an enzyme which is activated by F^- (Ross & Gilman, 1980), most enzymes which are affected exhibit strong inhibition by F^-. Several enzymes which are inhibited by F^- contain a heme-iron prosthetic group, and the F^- apparently serves as a sixth ligand to the iron. Such a complex has been identified for cytochrome *c* peroxidase (Yonetani, 1976) and catalase. The latter enzyme–F^- complex was shown to exhibit a F–Fe(III) hyperfine splitting and elicits a paramagnetic PRR enhancement (Vuk-Pavlović & Williams-Smith, 1977). Fluoride anion also elicits inhibition with several copper-containing proteins. The F^- has been shown to bind directly to a type 2 copper atom in laccase (Malkin et al., 1968; Brändén et al., 1971), ascorbate oxidase (Strothkamp & Dawson, 1977), and ceruloplasmin (Andréasson & Vänngard, 1970). Fluoride ion was also shown to bind to the Cu^{2+} of galactose oxidase (Marwedel et al., 1975) and to the Mn^{2+} of carboxypeptidase A (Navon et al., 1970).

The F^- anion inhibits AMP deaminase, apparently via interaction with the ATP effector site (Lee & Wang, 1968). The ligands F^- and P_i both inhibit succinate dehydrogenase in a competitive fashion and elicit a synergistic effect upon each other (Slater & Bonner, 1952) analogous to that observed for enolase (Warburg & Christian, 1941–1942; Wang & Himoe, 1974). The succinate dehydrogenase contains nonheme iron but does not use Mg^{2+} or Mn^{2+} in contrast to enolase. Furthermore, there is no phosphorylated substrate normally associated with this enzyme. The mechanism of the synergistic inhibition is not clear with succinate dehydrogenase. Fluoride also elicits potent inhibition of yeast pyrophosphatase in the presence of PP_i and Mg^{2+}. This "syncatalytic" inhibition apparently freezes the substrate as the covalent substrate–enzyme complex with tight binding of the F^- (Bayakov et al., 1976, 1977a,b). The fluoride ion possibly serves as an analogue of a hydroxyl ion which is a probable nucleophile in the catalytic reaction.

Fluoride ion was shown to be a potent inhibitor of enolase in the presence of the synergistic anion P_i (Warburg & Christian, 1941–1942). This observation accounted for the potent inhibition of glycolysis by this anion. Subsequent kinetic analyses have demonstrated that F^- or P_i alone serves as a weak inhibitor; but synergistically these anions serve as potent inhibitors of the enzyme with a 2:2:1 stochiometry. The inhibition is also cation dependent; inhibition is greater with Mg^{2+} than with Mn^{2+}, with little or no inhibition with Zn^{2+} (Wang & Himoe, 1974). Binding studies have demonstrated a direct interaction of these ligands to the enzyme–Mn^{2+} complex. The results quantitated the synergism of ligand interaction (Maurer & Nowak, 1981).

In the present study, the structural and kinetic parameters of the ternary and quaternary enolase–Mn complexes were studied by ^{19}F and ^{31}P relaxation rate measurements. The interaction of Mn^{2+} with F^- to form the Mn–F binary complex was first investigated. The dissociation constant for this complex was determined by measuring the concentration dependence of F^- on the paramagnetic effect of $1/T_1$ and $1/T_2$ and by an EPR titration of Mn^{2+}. The results yield a value of 0.30 ± 0.01 M. Since the value for $1/pT_{2p} \gg 1/pT_{1p}$, the value of $1/pT_{1p} = 1/T_{1M}$ for Mn–F. From the assumption that a 1:1 complex is formed and that a τ_c for the Mn–F [$Mn(H_2O)_5F$] complex is the same as that for the $Mn(H_2O)_6$ complex [2.9×10^{-11} s (Bloembergen & Morgan, 1961)], the Mn–F distance, r, can be calculated. With the assumption that the effect of T_1 relaxation for this complex is solely di-

polar, eq 6 can be used to calculate r. This calculation leads to a value of 1.92 ± 0.02 Å. This value is slightly shorter than the value of 2.12 Å determined crystallographically for the MnF_2 salt (Griffel & Stout, 1950). The relaxation rate values suggest a 1:1 complex in solution since a MnF_2 complex would yield a value for r from the above calculation of 1.72 Å. The shorter distance calculated from relaxation data (1.92 vs. 2.12 Å) may be due to some scalar interaction since the ligand observed is in direct contact with the Mn^{2+}. A temperature dependence of the relaxation rates of the binary complex was not performed. The value of $1/pT_{2p}$ may be $1/T_{2M}$ or $1/\tau_M$. This value may be a limit to $1/\tau_M$ therefore $1/pT_{2p} \geq 1/\tau_M = k_{off}$. Thus k_{off} for Mn–F $\geq 4.6 \times 10^6$ s^{-1}. This value is the same as that for water substitution on Mn^{2+} (5×10^6 s^{-1}). The second-order rate constant, k_{on}, calculated by assuming simple ligand exchange ($K_d = k_{off}/k_{on}$) gives $k_{on} \geq 1.5 \times 10^7$ M^{-1} s^{-1}.

The effect of enolase–Mn on ^{19}F relaxation was determined for the ternary enolase–Mn–F complex. The distribution of Mn^{2+} between the ternary complex and the binary Mn–F complex was determined by calculation with known dissociation constants. The $1/pT_{1p}$ for the ternary enzyme complex shows an enhancement compared to the binary complex. The $1/pT_{1p}$ is the largest relaxation rate observed for a Mn^{2+} ligand interaction to the authors' knowledge. These results conclusively demonstrate that the F^- ligand in the ternary enolase–Mn–F complex interacts directly with the bound Mn^{2+} in the formation of this complex. If we assume that at the highest temperatures where $1/pT_{1p}$ was observed (Figure 4), the slight curvature indicates a contribution from $1/T_{1M}$, a value for $1/T_{1M}$ can then be calculated. This value, calculated from such a slight deviation, would yield a value for $1/T_{1M}$ of 7.8×10^6 s^{-1} and r of 2.0 Å. The exchange rate for F^- from the ternary complex is 3.5×10^6 s^{-1}. This value is the same as the exchange rate of F^- from free Mn^{2+}.

The addition of P_i to form the quaternary E–Mn–F–P_i complex results in tighter F^- binding (Maurer & Nowak, 1981) and consequently a slower rate of ligand exchange. From a frequency dependence of ^{31}P relaxation in the same complex, >99% of the Mn^{2+} is in the quaternary complex. Thus the observed values for $1/pT_{1p}$ and $1/pT_{2p}$ do not require normalization for Mn^{2+} distribution. The identity of $1/pT_{1p}$ and $1/pT_{2p}$ and the negative slope of the Arrhenius plot (Figure 4) demonstrate that the relaxation rates reflect $1/\tau_M$ and give a lower limit to $1/T_{1M}$. The value for $1/pT_{1p}$ (Table 1) yields a value for $r < 4.3$ Å. Thus, the uncertainty in the Mn–F distance is greater in the quaternary complex. It is assumed, however, that the F^- does not change position relative to the bound Mn^{2+} upon formation of the quaternary complex but remains in the primary coordination sphere. The difference in relaxation rates is due to a decrease in k_{off} for the F^- ligand ($k_{off} = 4.5 \times 10^4$ s^{-1}) by 2 orders of magnitude, with an increase in the energy of activation of 0.6 kcal/mol for the F^- exchange. This decrease in k_{off} may be due to an additional interaction of the F^-, perhaps by hydrogen bonding, to a bound molecule of H_2O.

The interaction of P_i with enolase–Mn to form the respective ternary or quaternary complexes was investigated by ^{31}P relaxation rate studies. The P_i ligand has a greater affinity for Mn^{2+} than does F^- (1.9 mM vs. 300 mM). Thus the distribution of Mn^{2+} is an important consideration in an attempt to normalize the relaxation rate data. The K_d values of Mn^{2+} from the P_i-containing ternary and quaternary complexes were not independently known; therefore the Mn^{2+} distribution cannot be simply calculated. For evaluation of the Mn^{2+} distribution, a frequency dependence of the paramagnetic

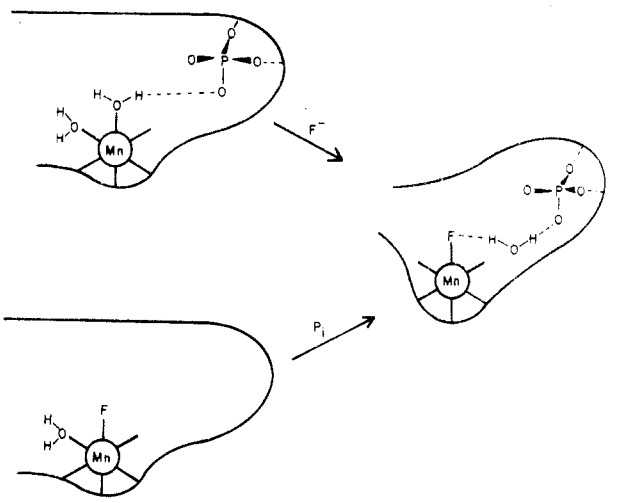

FIGURE 8: Structures of the enolase–Mn ternary and quaternary complexes. The figure demonstrates the structure of the ternary E–Mn–P_i complex with the P_i bound in a second sphere complex to the Mn^{2+} which is at the catalytic site. This site appears to be the same site occupied by the phosphoryl group of the substrate (Nowak et al., 1973). In the ternary E–Mn–F complex, the F^- ligand interacts in the first coordination sphere of the Mn^{2+}, displacing one of the two water molecules. In the quaternary E–Mn–F–P_i complex, a conformational change occurs which facilitates the binding of the Mn^{2+}, the F^-, and the P_i. The bound Mn^{2+} no longer has free access to the solvent, and the P_i moves further from the Mn^{2+}. It is postulated that the P_i may be linked to the bound F^- via an intervening water molecule held by hydrogen bonding.

effect, requiring a minimum of three frequencies, was shown to result in a determination of the distribution (see Materials and Methods). This approach is based on the assumption that the Mn–ligand effect is independent of frequency over the range measured. [The assumption will be true for Mn–ligand complexes where $\tau_c = \tau_r$ and the τ_r values are short ($1 + \omega_I^2\tau_c^2 \approx 1$).] This assumption can also be verified experimentally. An assumption is also made that τ_c for enzyme-bound Mn^{2+} and the ligand is frequency independent over the frequency range measured. This assumption is made for simplicity in calculation. Even if a maximum frequency dependence occurs, this can be accounted for. When such a correction was made for enolase complexes, no significant change in the results are obtained. From the frequency dependence of $1/T_{1M}$, a value for τ_c can also be obtained for the Mn–nuclear interaction.

The values for τ_c range approximately 4.0×10^{-9}–9.0×10^{-9} s with somewhat shorter τ_c values for the quaternary complex. The correlation functions [$f(\tau_c)$] show a smaller range of values [(4.3–5.9) $\times 10^{-9}$ s]. In the ternary complex, the calculated Mn–P_i distance of 6.5 Å precludes an inner sphere complex and suggests that the P_i forms a second sphere complex. This complex is consistent with P_i occupying the phosphoryl binding site of the substrate (Nowak et al., 1973). The addition of F^- adds a ligand to the bound Mn^{2+}, displaces a bound molecule of water, and perhaps "freezes" the remaining water molecule which is hydrogen-bonded to P_i. The conformational change of the enzyme, detected in the formation of this complex (Maurer & Nowak, 1981), results in P_i moving further away from the Mn^{2+} (7.7 Å).

No FPO_3^{2-} is formed under these conditions, as suggested by Warburg & Christian (1941–1942). With both F^- (0.1 M) and P_i (50 mM) incubated with enolase and Mn^{2+} for 72 h, no FPO_3^{2-} was shown to be formed as determined by ^{31}P NMR. A detection level of 5% was easily obtained.

The ligand exchange rates decrease in the quaternary complex. This data suggest that the decrease in k_{off} is enthalpicaly and entropically determined, suggesting a greater interaction

of the binding site of the protein with P_i. This site does not contain the cation. These results suggest that the quaternary enolase–Mn–F–P_i complex serves as a model for the transition state of the enzyme during catalysis. From kinetic isotope effects (DiNovo & Boyer, 1971; Shen & Westhead, 1973), the reaction proceeds via a carbocarbanion intermediate. Kinetic and NMR data indicate the first cation requirement acts to facilitate attack at C-3 of the substrate by activation of a water molecule (Nowak et al., 1973). The F^- appears to act as an OH^- analogue being isoelectronic with the hydroxyl ion, and the P_i occupies the phosphoryl site for the substrate. Figure 8 represents the structure of the enolase–Mn complexes which are formed upon the addition of the F^- and the P_i ligands.

The potency of inhibition of enolase and additional enzymes by F^- suggests that extreme care and reevaluation be made in the ingestive use of F^- as an additive for prophylaxis of dental caries.

References

Allerhand, A., Doddrell, D. Glushko, V., Cochran, D. W., Wenkert, E., Lawson, P. J., & Gurd, F. R. N. (1971) *J. Am. Chem. Soc. 93*, 544–546.

Andrēasson, L.-E., & Vänngard, T. (1970), *Biochim. Biophys. Acta 200*, 247–254.

Bayakov, A. A., Artjukov, A. A., & Avaeva, S. M. (1976) *Biochim. Biophys. Acta 429*, 982–992.

Bayakov, A. A., Artjukov, A. A., & Avaeva, S. M. (1977a) *Biochim. Biophys. Acta 481*, 195–201.

Bayakov, A. A., Bakuleva, N. P., Nazarova, T. I., & Avaeva, S. M. (1977b) *Biochim. Biophys. Acta 481*, 184–194.

Bloembergen, N. (1957) *J. Chem. Phys. 27*, 572–573.

Bloembergen, N., & Morgan, L. O. (1961) *J. Chem. Phys. 34*, 842–850.

Brändēn, R., Malmström, B. G., & Vänngard, T. (1971) *Eur. J. Biochem. 18*, 238–241.

Cohn, M., & Townsend, J. (1954) *Nature (London) 173*, 1090–1091.

DiNovo, E. C., & Boyer, P. D. (1971) *J. Biol. Chem. 246*, 4586–4593.

Griffel, M., & Stout, J. W. (1950) *J. Am. Chem. Soc. 72*, 4351–4356.

Hanlon, D. P., & Westhead, E. W. (1969) *Biochemistry 8*, 4247–4255.

Keirns, J. J., Kreiner, P. W., Brock, W. A., Freeman, J., & Bitensky, M. W. (1973) *Miami Winter Symp.*, 181–205.

Lee, Y.-P., & Wang, M. H. (1968) *J. Biol. Chem. 243*, 2260–2265.

Luz, Z., & Meiboom, S. (1964) *J. Chem. Phys. 40*, 2686–2692.

Malkin, R., Mälmstrom, B. G., & Vänngard, T. (1968) *FEBS Lett. 1*, 50–54.

Mann, K. G., Castellino, F. J., & Hargrave, P. A. (1970) *Biochemistry 9*, 4002–4007.

Marwedel, B. J., Kurland, R. J., Kosman, D. J., & Ettinger, M. J. (1975) *Biochem. Biophys. Res. Commun. 63*, 773–779.

Maurer, P. J., & Nowak, T. (1981) *Biochemistry* (preceding paper in this issue).

Mildvan, A. S., & Cohn, M. (1970) *Adv. Enzymol. Relat. Areas Mol. Biol. 33*, 1–70.

Mildvan, A. S., & Engle, J. (1972) *Methods Enzymol. 26C*, 654–682.

Mildvan, A. S., Leigh, J. S., Jr., & Cohn, M. (1967) *Biochemistry 6*, 1805–1818.

Navon, G., Shulman, R. G., Wyluda, B. J., & Yamane, T. (1970) *J. Mol. Biol. 51*, 15–30.

Nowak, T. (1978) *Arch. Biochem. Biophys. 186*, 343–350.

Nowak, T., & Lee, M. J. (1977) *Biochemistry 16*, 1343–1349.

Nowak, T., Mildvan, A. S., & Kenyon, G. L. (1973) *Biochemistry 12*, 1690–1701.

Ross, E. M., & Gilman, A. G. (1980) *Annu. Rev. Biochem. 49*, 533–564.

Shen, T. Y. S., & Westhead, E. W. (1973) *Biochemistry 12*, 3333–3337.

Slater, E. C., & Bonner, W. D. (1952) *Biochem. J. 52*, 185–196.

Solomon, I. (1955) *Phys. Rev. 99*, 559–565.

Strothkamp, R. E., & Dawson, C. R. (1977) *Biochemistry 16*, 1926–1929.

Swift, T., & Connick, R. (1962) *J. Chem. Phys. 37*, 307–320.

Vold, R. L., Waugh, J. S., Klein, M. P., & Phelps, D. E. (1968) *J. Chem. Phys. 48*, 3831–3832.

Vuk-Pavolic, S., & Williams-Smith, D. L. (1977) *Biochemistry 16*, 5465–5470.

Wang, T., & Himoe, A. (1974) *J. Biol. Chem. 249*, 3895–3902.

Warburg, O., & Christian, W. (1941–1942) *Biochem. Z. 310*, 384–421.

Westhead, E. W., & McLain, G. (1964) *J. Biol. Chem. 239*, 2464–2468.

Yonetani, T. (1976) *Enzymes, 3rd Ed. 13*, 345–361.